THE JOURNAL OF BIOLOGICAL CHEMISTRY
Vol. 274, No. 52, Issue of December 24, pp. 37259–37264, 1999
Printed in U.S.A.

The Structural Basis for the Increased Immunogenicity of Two HIV-Reverse Transcriptase Peptide Variant/Class I Major Histocompatibility Complexes*

(Received for publication, June 25, 1999, and in revised form, August 24, 1999)

Timothy J. Kirksey‡, Rebecca R. Pogue-Caley‡§, Jeffrey A. Frelinger‡, and Edward J. Collins‡¶‖

From the ‡Department of Microbiology and Immunology and the ¶Department of Biochemistry and Biophysics, the University of North Carolina, Chapel Hill, North Carolina 27599

Designing altered peptide ligands to generate specific immunological reactivity when bound to class I major histocompatibility complexes is important for both therapeutic and prophylactic reasons. We have previously shown that two altered peptides, derived from human immunodeficiency virus (HIV)-reverse transcriptase (RT) residues 309–317, are more immunogenic *in vitro* than the wild-type peptide. One peptide variant, I1Y, was able to stimulate RT-specific cytotoxic T cells from the blood of three HIV-infected individuals better than the wild-type RT peptide. Both I1Y and I1F peptide variants increase the cell surface half-life of the peptide-class I complex approximately 3-fold over that of the RT peptide but have different immunological activities. These peptides are candidates for the design of vaccines for HIV due to their increased immunogenicity. To understand the basis for the increased cell surface stability compared with wild-type peptide and to understand the differences in T cell recognition between I1Y and I1F, we determined the x-ray crystal structures of the two class I MHC-peptide complexes. These structures indicate that the increased cell surface half-life is due to π-π stacking interactions between Trp-167 of HLA-A2.1 and the aromatic P1 residues of I1F and I1Y. Comparison of the structures and modeling potential T cell receptor (TCR) interactions suggests that T cell interactions and immunogenicity are different between I1Y and I1F for two reasons. First, subtle changes in the steric and polar properties of the I1Y peptide affect TCR engagement. Second, water-mediated hydrogen bond interactions between the P1-Tyr and the P4-Glu peptide residues increase peptide side chain rigidity of residues critical for TCR engagement.

The cytolytic immune response is a major component of the body's defense against viral infection (1). This response is mediated by the interaction between the T cell receptor (TCR)[1] on $CD8^+$ cytotoxic T lymphocytes (CTLs) and the class I major histocompatibility complex (MHC) molecules expressed on the surface of antigen-presenting cells (2). Control of viral infections such as HIV requires a vigorous CTL response (3).

Class I MHC molecules are trimolecular complexes consisting of an allotype-specific heavy chain, a light chain β_2-microglobulin, and an endogenously processed peptide. The antigenic peptide typically binds with the termini buried in the peptide-binding cleft. The middle of the peptide frequently bulges out of the peptide-binding cleft. Bulging in the center makes these residues more accessible to the TCR and as such these residues are usually critical for TCR recognition (see Ref. 4 for review).

Class I MHC molecules are capable of binding a diverse set of peptides with long half-lives. A major component of the binding energy is derived from interactions between conserved residues in the peptide-binding cleft and the invariant peptidic termini (5). Additionally, peptides that bind with high affinity typically have two or more relatively invariant residues, termed anchors, that bind in specificity pockets primarily composed of class I heavy chain polymorphic residues (6–8). Other positions in the peptide can also make significant contributions to peptide-MHC affinity (9).

Previously, we identified two aromatic single amino acid substitutions at the amino-terminal end (P1 position, normally isoleucine) of the HLA-A2.1 (A2)-restricted HIV reverse transcriptase (RT) peptide-(309–317) (ILKEPVHGV) that increase the cell surface half-lives of complexes 3-fold over the A2/RT-peptide complex. These two peptides, designated I1F and I1Y, also show increased immunogenicity compared with the wild-type RT. *In vitro* experiments with peripheral blood lymphocytes (PBLs) from three different HIV-positive patients show that *in vitro* expansion of CTL using I1Y-pulsed antigen-presenting cells stimulates a higher CTL response against wild-type RT-pulsed target cells than *in vitro* expansion with the RT peptide itself. In contrast, I1F-pulsed cells stimulate a higher response against RT-pulsed cells in only one of the two sets of donor PBLs that were tested. The I1F and I1Y peptides also differ in their ability to be recognized by RT-specific CTL lines (10).

To understand better why the I1Y, I1F, and RT peptides have differing immunological properties, we determined the x-ray crystal structures of A2 complexed with I1Y and I1F peptides to 2.2 and 2.8 Å resolution, respectively. Comparison of these structures with the previously determined RT structure (5), along with modeling the interactions of the A6 and B7

* This research was supported by National Institutes of Health Grants A120288 and A129324. The costs of publication of this article were defrayed in part by the payment of page charges. This article must therefore be hereby marked "*advertisement*" in accordance with 18 U.S.C. Section 1734 solely to indicate this fact.

The atomic coordinates and structure factors (codes 1I1Y and 1I1F) have been deposited in the Protein Data Bank, Research Collaboratory for Structural Bioinformatics, Rutgers University, New Brunswick, NJ (http://www.rcsb.org/).

§ Current address: Dept. of Immunology, Duke University, Durham, NC 27710

‖ To whom correspondence should be addressed: Dept. of Microbiology and Immunology, The University of North Carolina, CB 7290, 804 M. E. Jones Bldg., Chapel Hill, NC 27599-7290. Tel.: 919-966-6869; Fax: 919-962-8103; E-mail: collins1@med.unc.edu.

[1] The abbreviations used are: TCR, T cell receptor; RT, reverse transcriptase; MHC, major histocompatibility complex; HIV, human immunodeficiency virus; CTL, cytotoxic T lymphocytes; PBLs, peripheral blood lymphocytes; MES, 4-morpholineethanesulfonic acid; NCS, noncrystallographic-symmetry; r.m.s., root mean square.

TCRs (11, 12) with the three A2 structures, has given us insight into the differing immunological properties. The crystallographic structures suggest that the increases in cell surface half-life are due to interactions between the aromatic P1 residues (Tyr and Phe) and tryptophan-167 of A2. Pseudo homology models of TCR and these class I MHC complexes suggest that the differences in T cell recognition between the I1Y and I1F complexes may be attributed to two subtle structural differences due specifically to the hydroxyl group of P1-tyrosine.

MATERIALS AND METHODS

Synthetic Peptides—All peptides were synthesized by the Peptide Synthesis Facility at the University of North Carolina, Chapel Hill. The sequences of the peptides are ILKEPVHGV (wild-type RT), YLKEPVHGV (I1Y), and FLKEPVHGV (I1F). All peptides were purified by reverse-phase high pressure liquid chromatography to greater than 95% purity, and the sequences were confirmed by matrix-assisted laser desorption ionization-time of flight spectrometry.

Folding and Purification of A2 Complexes—A2/I1Y and A2/I1F complexes were folded by rapid dilution *in vitro* as described previously (13). After incubation for 36–48 h at 10 °C, the folding solutions were concentrated in an ultrafiltration cell (Amicon; Beverly, MA) and purified by high pressure liquid chromatography-gel filtration chromatography (Phenomenex, BioSep-SEC-S2000) in 50 mM Tris-Cl, pH 7.5, 150 mM NaCl. Purified complexes were then concentrated using Centricon-10 concentrators (Amicon) and exchanged into buffers consisting of either 25 mM MES, pH 6.5, for crystallization, or 10 mM potassium phosphate, pH 7.4, for circular dichroism experiments.

Thermal Stability of A2 Complexes—The relative stabilities of the peptide/A2 complexes were measured by circular dichroism (CD) thermal denaturation experiments. The experiments were performed on an AVIV 62-DS spectropolarimeter equipped with a Peltier temperature control unit. The protein concentration was approximately 10 μM in 10 mM potassium phosphate, pH 7.4. The thermal denaturation of purified A2/RT, A2/I1Y, and A2/I1F complexes was monitored as the change in circular dichroic signal at 218 nm from 4 to 95 °C. The T_m values (50% denatured) were determined by modeling the denaturation as a two-state process (14) from a normalized plot of the denaturation. The reported T_m is the average of three separate thermal denaturation experiments. The error associated with the reported T_m is the sum of the machine error (0.5 °C) and the error in the curve fit (~0.5 °C).

Crystallization—Both A2/I1Y and A2/I1F complexes were crystallized by the hanging drop vapor-diffusion method. The well solution for A2/I1Y contained 18% PEG-8000 in 25 mM MES, pH 6.5, and the hanging drop was a 1:1 mixture of the well solution and 10 mg/ml protein in 25 mM MES, pH 6.5. The well solution for A2/I1F contained 20% PEG-8000 in 25 mM MES, pH 6., and the hanging drop was a 1:1 mixture of the well solution and 10 mg/ml protein in 25 mM MES, pH 6.5. Microseeding was performed for both complexes to obtain large single crystals suitable for crystallographic studies.

Data Collection and Processing—Crystals were transferred directly into cryoprotectant buffer containing 20% PEG-8000 supplemented with 25–30% glycerol in 25 mM MES, pH 6.5, and placed directly into a 100 K nitrogen stream generated by an Oxford Cryo System. The A2/I1Y diffraction data were collected on beamline X-12B at the National Synchrotron Light Source (NSLS), Brookhaven National Laboratories (Upton, NY). The A2/I1F diffraction data were collected on a Rigaku R-Axis IIC using CuK_α radiation. All diffraction data were processed using the programs Denzo and Scalepack (15). Data statistics are shown in Table I.

Structure Determination—The structures of both complexes were determined using the Molecular Replacement method (AMoRe) with the CCP4 program suite (16) using the A2/hepatitis B virus nucleocapsid peptide-(18–27) (FLPSDFFPSV) crystallographic structure (5) as the search model (Protein Data Bank code PDB1HHH). As there are two molecules per asymmetric unit of each crystal, 2-fold non-crystallographic averaging coupled with solvent flattening and histogram matching (DM) (17) greatly improved the quality of the electron density maps. Manual model building into the electron density maps was performed using the program O (18).

Refinement of A2/I1Y—Computational refinement was performed using the programs X-PLOR version 3.851 (19) and Refmac (20) in CCP4 (21). The structure was first refined in X-PLOR using 8–2.2-Å resolution data. Two-fold non-crystallographic-symmetry (NCS) restraints were applied to the two molecules in the asymmetric unit of A2/I1Y crystals with a weight of 300 kcal mol^{-1} $Å^{-2}$. Overall isotropic B factor refinement was first performed, followed by rigid body refinement using three structural domains as follows: $\alpha 1/\alpha 2$ (the peptide-binding superdomain), $\alpha 3$, and β_2-microglobulin. Cycles of computational refinement were performed using positional refinement. Later cycles of refinement were performed using Refmac with "strict" NCS restraints (see Refmac manual), a bulk solvent correction, overall anisotropic B factor correction, and individual B factor refinement. 192 water molecules were added to the structure using program ARP (22) in CCP4 with Refmac as the refinement tool. The final R_{free} (23) and R_{work} factors ($F > 0$) between 30 and 2.2 Å are 28.9 and 24.4%, respectively. The refinement statistics are shown in Table I.

The conformations of the peptides were confirmed by the following "averaged" omit map procedure. The peptide was omitted from the refined model before calculation of the phases and structure factors used to generate the electron density map input into DM. Model masks were made using peptide to be sure that all averaging included peptide regions. Finally, model phase bias was reduced from the initial map in DM by 2-fold non-crystallographic averaging, solvent flattening, and histogram matching.

Refinement of A2/I1F—Refinement of A2/I1F was performed as was A2/I1Y except Refmac was used throughout the refinement. Rigid body refinement was used to optimize the domain positions. Cycles of positional refinement were performed with strict NCS restraints (see Refmac manual), a bulk solvent correction, overall anisotropic B factor correction, and overall temperature factor refinement. Final cycles included individual temperature factor refinement. This was justified by

TABLE I
Summary of crystallographic statistics

Parameters	A2/I1Y	A2/I1F
Space group	P1	P1
Cell dimensions	a = 50.61 Å	a = 49.57 Å
	b = 63.59 Å	b = 62.97 Å
	c = 75.33 Å	c = 74.56 Å
	α = 81.93 °	α = 82.08 °
	β = 75.94 °	β = 76.47 °
	γ = 78.00 °	γ = 77.78 °
Molecules/AU	2	2
Resolution (Å)	2.2	2.8
Number of crystals	1	1
R_{merge} (%)[a]	7.3 (23.1)[b]	11.0 (32.0)
<I/G>	9.70 (2.60)	13.2 (4.1)
Unique reflections	45024	21030
Total observations	222078	148065
Completeness (%)	97.9 (96.4)	99.2 (98.6)
Refinement ($F > 0$)		
Resolution (Å)	30–2.2 Å	15–2.8 Å
R_{work}[c] (no. of reflections)	24.4% (40,341)	27.4% (18,619)
R_{free} (no. of reflections)	28.9% (3600)	31.5% (2102)
No. of non-hydrogen atoms	6316	6315
No. of water molecules	192	NA[f]
Average B factor	21.7	43.2
<RSCC>[d]	87.3%	74.5%
Error[e]	0.20 Å	0.42 Å
r.m.s. deviations from ideality		
Bonds (Å)	0.010	0.009
Angles (°)	2.489	2.493
Dihedrals (°)	25.433	26.095
Impropers (°)	1.724	1.907
Residues in Ramachandran plot (%)		
Most favored	91.7	89.0
Additional allowed	8.0	10.6
Generously allowed	0.3	0.4
Disallowed	0	0

[a] $R_{merge}=\Sigma_{hkl}\ \Sigma_i\ |I_i - I|/\Sigma_{hkl}\ \Sigma_i\ I_i$, where I_i is the observed intensity and is the average intensity of multiple observations of symmetry related reflections.

[b] Number in parentheses refers to the highest resolution shell.

[c] $R=\Sigma_{hkl}\ |F_{obs}|-k|F_{cal}|\ |/\Sigma_{hkl}\ |F_{obs}|$, where R_{free} is calculated for a randomly chosen 8% of reflections; R_{work} is calculated for the remaining 92% of reflections used for structure refinement.

[d] Real space fit correlation coefficient calculated in O (17).

[e] Error is the mean estimate of the positional error based on maximum likelihood methods calculated in Refmac (20).

[f] NA, not applicable.

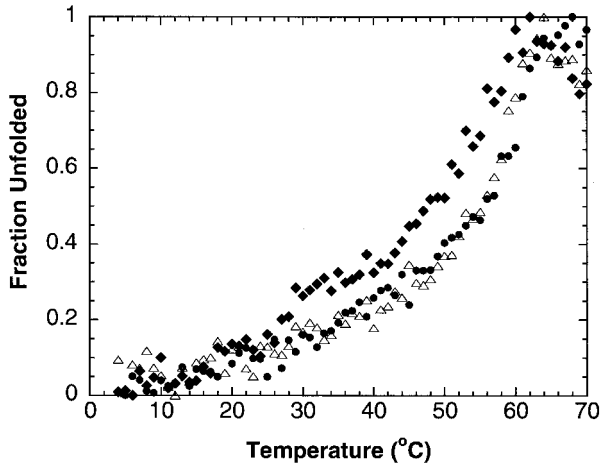

FIG. 1. **Circular dichroism experiments show that the I1F and I1Y peptides stabilize A2 to higher temperatures than does RT.** The relative stabilities of the peptide-MHC complexes were measured by circular dichroism thermal denaturation experiments. The thermal denaturation of purified A2/RT (♦), A2/I1Y (●), and A2/I1F (△) complexes (~10 μM) was monitored as the change in circular dichroic signal at 218 nm from 4 to 95 °C. The T_m values (50% denatured) were determined modeling the denaturation as a two-state process (14).

the observation of a drop in the R_{free}. The final R_{free} and R_{work} factors ($F > 0$) between 15 and 2.8 Å are 31.5 and 27.4%, respectively. The refinement statistics are shown in Table I.

RESULTS

Relative Thermal Stability by Circular Dichroism (CD) Analysis—The thermal stability of class I MHC molecules, as measured by circular dichroism (CD), is proportional to the free energy of peptide binding (24). We used CD thermal denaturation experiments to compare the relative thermal stability of purified A2 folded *in vitro* with I1Y, I1F, and RT peptides. A2/I1F and A2/I1Y complexes generated significantly higher melting temperatures (temperature at which 50% of the complexes have denatured) at 55 and 56 °C, respectively, compared with 48 °C for A2/RT (Fig. 1). Therefore, both I1F and I1Y peptides bind to A2 with higher affinity than RT. These results are consistent with the increased cell surface half-lives we have previously reported (10). In order to understand why they bind with higher affinity, we determined their crystal structures bound to A2.

Crystal Structures of A2/I1Y and A2/I1F—The x-ray crystal structures of the A2/I1Y and A2/I1F complexes were determined to a resolution of 2.2 and 2.8 Å, respectively. Both structures show clear, unambiguous density throughout the model. Overall, the A2/I1Y and A2/I1F structures are very similar to the RT structure (5) (r.m.s. deviations of 0.33 Å each when superpositioning the α-carbons of the peptide-binding super domains). The peptide positions are unambiguous in the density. The averaged omit maps for the I1Y and I1F peptides (see under "Materials and Methods") are shown in Fig. 2, *A* and *B*. Both the I1Y and I1F peptides bind in the cleft in a conformation similar to that of the RT peptide, as shown in Fig. 2, *C* and *D*. The I1Y and I1F peptides have r.m.s. deviations of 0.33 Å and 0.25 Å for the α-carbon backbone of the peptides alone, respectively, based on the above superimposition of the α1/α2 domains onto the A2/RT α1/α2 domains.

Upon completion of the crystal structure determinations, we looked for a reason for the increased affinity of the I1F and I1Y peptides as compared with RT. As the overall structures of the complexes are identical, we examined the peptides. In general, the paths of the main chain atoms of the peptides are identical. The side chain orientations of the P1 residues of the three peptides are similar, with the side chain pointing out of the binding cleft toward the TCR (Fig. 2, *C* and *D*). The aromatic rings of phenylalanine and tyrosine of I1F and I1Y are both oriented parallel to tryptophan-167 of the A2 binding cleft at a distance of 3.5 Å, suggesting these P1 substitutions allow stabilizing π-π orbital interactions with tryptophan-167. These π-π stabilizing interactions are not possible with the isoleucine in the wild-type peptide. The interaction of the P1 residue of I1Y peptide with tryptophan-167 is shown in Fig. 3*B*.

Next, we asked why T cell recognition is increased for the A2/I1F and A2/I1Y complexes compared with A2/RT. Examination of the structures shows one significant topological change to the surface of the TCR contact region when compared with the A2/RT complex. The P1 side chains I1Y and I1F protrude farther out of the peptide-binding cleft. The increased size of these amino acids increases the distance that the P1 side chain protrudes from the binding cleft by 2.9 and 1.6 Å, respectively.

The only other difference between the structures of the I1Y peptide and the RT peptide, besides the substitution at the first position, is at the P4 glutamate. In the A2/I1Y structure, the P4 glutamate moves 0.6 Å from the RT position toward the P1 tyrosine. The distance between the tyrosine hydroxyl and the carboxylate of the glutamate is 5.7 Å and is too long for a direct hydrogen bond. The averaged omit map shows an elongated stretch of electron density perpendicular to the peptide backbone between the P1 and P4 residues, as shown in Fig. 4. This region of density is large enough to accommodate up to three waters at various occupancies. A water molecule within this stretch of electron density would be sufficient to bridge a hydrogen bond interaction between the tyrosine and the glutamate. However, the relatively low peak heights in the electron density maps suggest that these waters are not highly occupied. The side chain nitrogen of lysine-66 in the A2 binding cleft is sufficiently close to participate in a hydrogen bond with a water molecule that lies between the P1 and P4 residue as well. Conversely, in the I1F structure the glutamate at position 4 moves 1.1 Å (relative to the RT position) toward the carboxyl-terminal end of the peptide. Thus, the overall effect is to either move the glutamate side chain toward the potential hydrogen-bonding partner at P1 (in I1Y) or away from P1 (in I1F).

Modeling of TCR Interactions—In order to understand the potential effects that the P1 substitutions would have on TCR recognition, we modeled the P1 residues at the TCR/class I interface. There is close similarity at P1-P2 of the Tax peptide (leucine-leucine) in the TCR-MHC co-crystal structure (11, 12) and the RT peptide (isoleucine-leucine). Therefore, the structures of human αβ TCRs A6 (11) and B7 (12), both co-crystallized with A2/Tax peptide (LLFGYPVYV), provide a good model for comparing the TCR-MHC interactions between RT and I1Y/I1F. Both TCRs were modeled onto the A2/I1Y, A2/I1F, and A2/RT structures by superimposing the α1/α2 domains of our structures onto the α1/α2 domains of A2/Tax complex in each of the co-crystal structures. The r.m.s. deviations for the superimposition of the A2/TOX molecules in the A6 and B7 TCR co-crystal structures onto A2/RT were 0.50 and 0.42 Å. A model of the B7 TCR docked with A2/I1Y is shown in Fig. 3*A*. Interatomic distances were calculated between the P1 peptide residue and the nearest residue of the TCR and are summarized in Table II.

There are no unfavorable van der Waals contacts between the P1 isoleucine of RT and the two TCRs. However, the phenylalanine of A2/I1F, makes one significantly bad van der Waals contact with methionine 28 of the B7-TCR (2.11 Å as compared with the optimal value of 3.4 Å). All of the potential bad contacts of I1F with the A6 TCR are within experimental

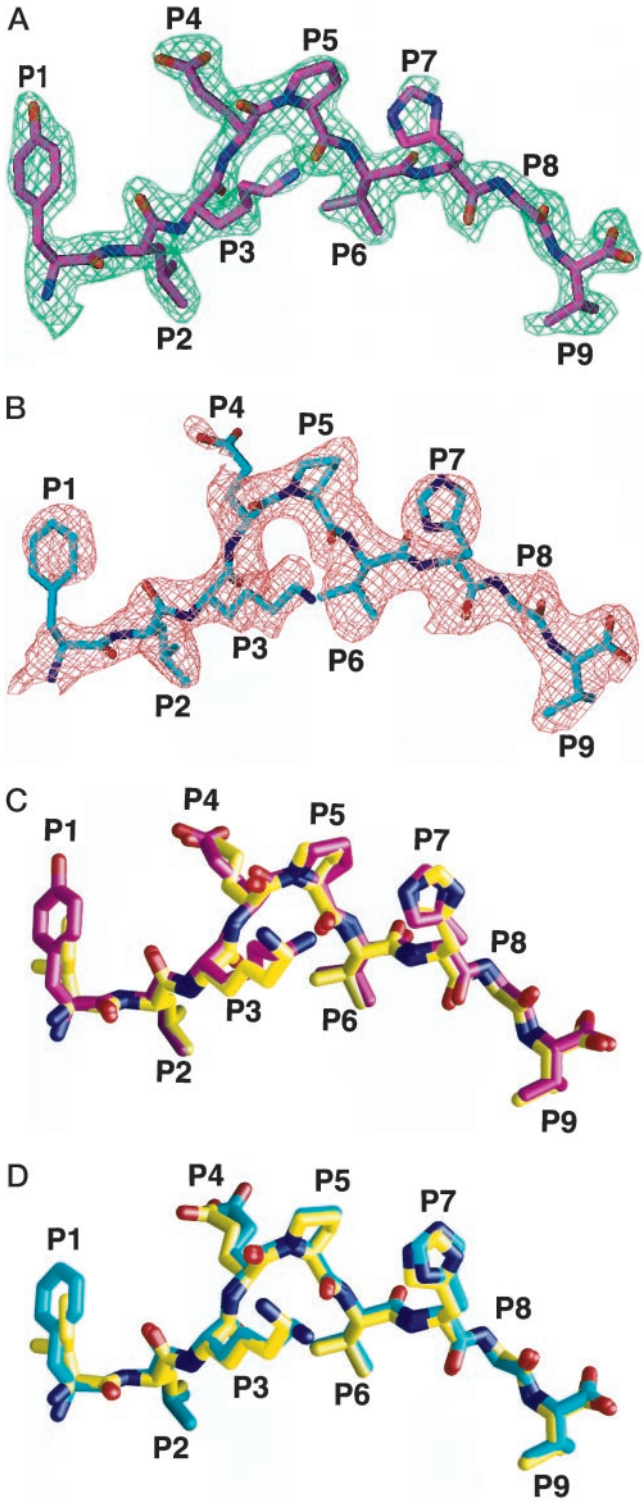

FIG. 2. **I1Y and I1F peptides assume the same main chain conformations as the RT peptide within the peptide-binding cleft of A2.** The A2-binding cleft residues are omitted for clarity. The orientation of the peptides is with the α2-helix in front of the plane of the page, the α1-helix behind the plane of the page, and the β-sheet domain below the peptide. *A,* 2 $F_o - F_c$ averaged omit map of I1Y peptide at a contour level of 1.4 σ and a cover radius of 1.4 Å. *B,* $2F_o - F_c$ averaged omit map of I1F peptide at a contour level of 0.9 σ and a cover radius of 1.4 Å. *C* and *D,* the α1/α2 domains of A2/I1Y and A2/I1F were superimposed onto the α1/α2 domain of the A2/RT structure (5), with r.m.s. deviation values of 0.33 and 0.33 Å, respectively. Based on this same superimposition, the r.m.s. deviation values for the α-carbon backbone of the I1Y and I1F peptides relative to the RT peptide are 0.33 and 0.25 Å, respectively. *C,* comparison of the I1Y peptide (*magenta*) and the RT peptide (*yellow*). *D,* comparison of the I1F peptide (*cyan*) and the RT peptide (*yellow*).

error. The additional hydroxyl of the tyrosine side chain (I1Y), as compared with I1F, increases the number of unfavorable van der Waals contacts to five for the B7-TCR and three for the A6-TCR. Collectively, these data suggest that the B7 and A6 TCR would not bind to these complexes because of the unfavorable van der Waals contacts brought by the larger phenylalanine and tryrosine side chains. This is not unexpected because the A6 and B7 TCR are not known to recognize A2/RT or RT-variant peptide complexes. But, these data do suggest that RT-specific TCRs could take advantage of these larger (and for I1Y, more polar) P1 side chains to increase the TCR binding affinity for the A2/I1Y and A2/I1F complexes.

DISCUSSION

The design of peptides with high affinity for class I MHC to use in peptide-based vaccines requires a process of molecular "fine-tuning." In this process, the peptide must be altered in a manner significant enough to increase the affinity of peptide for MHC, but these changes must be also be subtle enough so that the peptide-MHC complex is still recognized by the repertoire of TCRs that recognize wild-type peptide. Increases in immunogenicity may be accounted for by the following three non-exclusive mechanisms. 1) Changes to the peptide that increase the stability of the peptide-MHC complex increase the cell surface half-life of the complex. This would increase the relative concentration of the peptide-MHC complex at the cell surface and by standard equilibrium processes increase the number of engaged MHC/TCR. 2) The increased concentration of the complexes at the cell surface and association with the membrane increases the avidity of the MHC-TCR interaction. 3) Changes in the peptide directly increase the affinity (or duration of contact) of the peptide-MHC complex for TCR. In this study, we have seen examples of all of these mechanisms.

We previously screened 11 different P1 substitutions of the HIV-RT peptide for the ability to increase the A2/peptide complex stability at the cell surface (10). P1 substitutions were chosen in an effort to minimize alterations in T cell interactions, given that structural data suggest the majority of the P1 residue is typically buried in the binding cleft (5). Two P1 substitutions, I1F and I1Y, increased the cell surface half-life of the A2/peptide complex from 10 to 30 h (10). I1Y stimulated a higher CTL response against wild-type RT-pulsed target cells than the RT peptide itself.

These investigations raise several structural questions regarding the differing immunological properties between A2/RT, A2/I1Y, and A2/I1F complexes. First of all, what features of the A2/I1Y and A2/I1F complexes account for the drastic increase in cell surface half-life? Second, how do we account for the difference in immunogenicity of the two peptides, given that the cell surface half-lives of the A2/I1Y and A2/I1F complexes are nearly identical? Finally, how do we account for the differences in RT-specific CTL line recognition between I1Y and I1F? To understand better the structural basis for the differing immunological properties between A2/RT, A2/I1Y, and A2/I1F complexes, we determined the x-ray crystal structures of the A2/I1Y and A2/I1F complexes at 2.2- and 2.8-Å crystallographic resolution, respectively. The 2.5-Å structure of A2/RT was described previously by Madden *et al.* (5) and is used for comparison with our models.

Biochemically, one of the striking differences between the A2/RT and both the A2/I1Y and A2/I1F complexes is the dramatic increase in cell surface half-life. A significant feature revealed in the A2/I1Y and A2/I1F crystal structures is the parallel orientation of the aromatic P1 residues and Trp-167 at a distance of 3.5 Å, which defines the peptide amino-terminal end of the binding cleft (Fig. 3). Aromatic-aromatic interactions

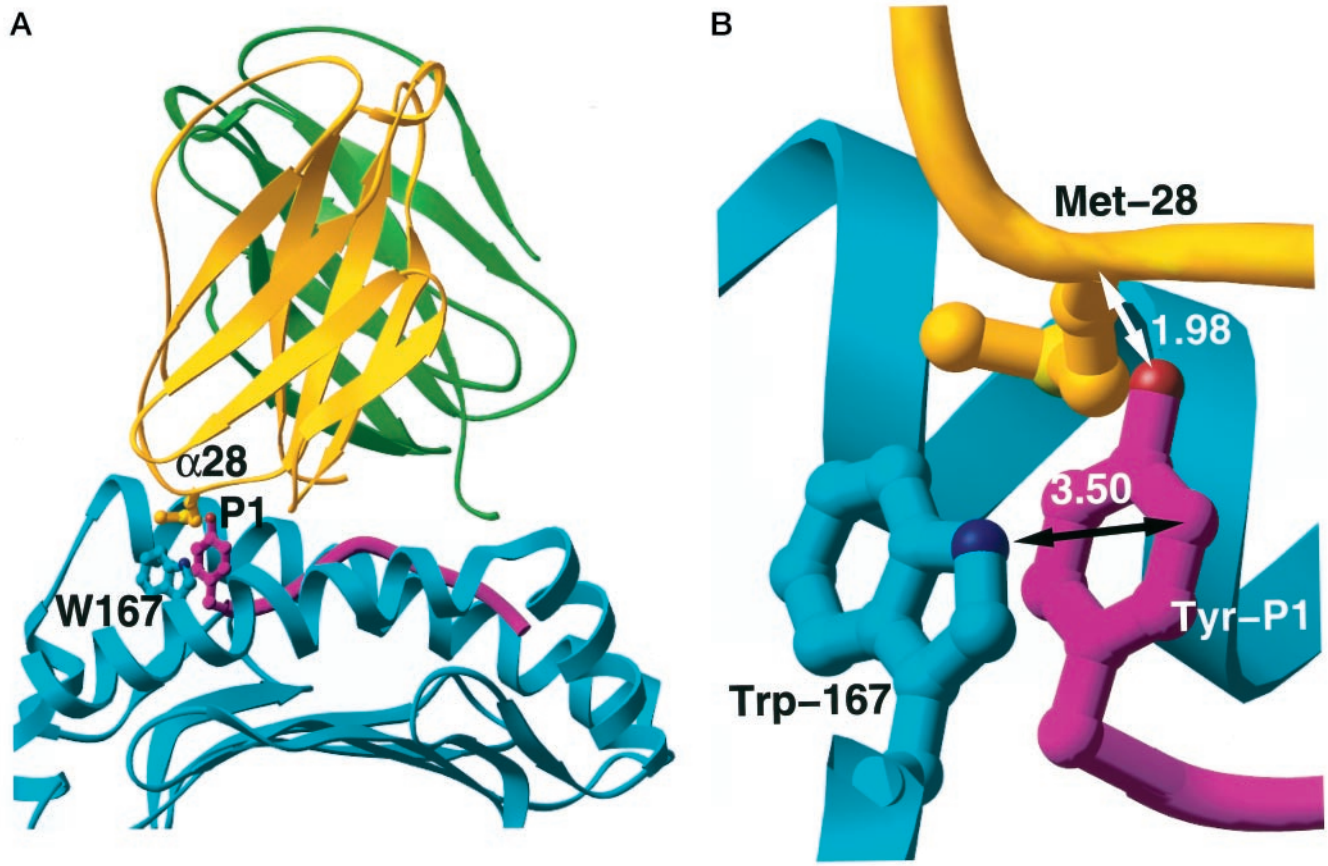

FIG. 3. **The P1 tyrosine of the A2/I1Y complex forms π-π stacking interactions with Trp-167 of A2 and has extensive contacts with Met-28 in the CDR1α loop of the B7 TCR.** A portion of the α chain (*yellow*) and β chain (*green*) of B7 TCR is modeled onto the α1/α2 domain of A2 (*cyan*) and bound I1Y peptide (*magenta*) complex, as described under "Materials and Methods." *A,* overall view of B7 TCR docked with the A2/I1Y complex. *B,* enlarged view showing the interactions of P1-Tyr (*magenta*) with Trp-167 of A2 (*cyan*) and Met-28 of the B7 TCR (*yellow*). The aromatic moiety of P1-Tyr (*magenta*) forms a stabilizing π-π orbital interaction with Trp-167 (*cyan*). The hydroxyl moiety of P1-Tyr makes extensive contacts with Met-28 (*yellow*) of the B7 TCR. The distance shown is for the interaction of the P1-Tyr hydroxyl to the α-carbon of Met-28. This interaction is one of five unfavorable van der Waals interactions between the two residues (summarized in Table II). All distances are in Å.

are a common mechanism in protein stabilization and are estimated to contribute −1 to −2 kcal/mol binding energy (25). It is likely that this feature of the A2/I1F and A2/I1Y complexes accounts for the increased cell surface half-lives of the peptide-MHC complexes. This is consistent with the 7–8 °C increase in thermal stability observed in the CD thermal denaturation experiments with the A2/I1F and A2/I1Y complexes.

The increase in cell surface half-life of the A2/I1Y complex is probably an important determinant with respect to the increased immunogenicity of A2/I1Y. The primary mechanism could be postulated to be that the increase in the concentration of the complex at the cell surface increases the potential number of class I complexes that interact with the TCR by thermodynamic mechanisms. But it cannot be the entire story. Both A2/I1Y and A2/I1F complexes have identical cell surface half-lives of 30 h (compared with 10 h for the RT complex). However, in *in vitro* experiments using PBLs from HIV-positive donors, the I1Y peptide was able to stimulate a higher CTL response against RT-specific target cells than RT peptide stimulation itself in three of three PBL sets tested. On the other hand, I1F stimulated a higher CTL response in the PBLs of only one of the two donors tested. Changes to the affinity and/or duration of contact between MHC-peptide and TCR must be involved. There are two potential explanations for this phenomenon. The first explanation is that all the TCRs of the T cells that respond to A2/RT have increased affinity for (or prolong contact with) A2/I1Y. It could also be that only a subset of T cells actually respond to A2/I1Y, but the TCR have higher affinity for (or prolonged contact with) A2/I1Y, and that interaction makes the subset of T cells respond better then the full set of T cells to A2/RT. Unfortunately, we cannot resolve these two possibilities because the cell lines are extinct, and the donors are deceased.

Our crystallographic studies reveal that the A2/I1Y complex has two significant structural differences from the RT and I1F complexes that could affect TCR interactions. From our modeling studies with the A6 and B7 TCRs onto the A2/RT, A2/I1F, and A2/I1Y complexes, it is evident that the P1-Tyr of the bound I1Y peptide protrudes far enough out of the binding cleft to make significant unfavorable contacts with residues of the TCR (Fig. 3). However, in the T cell repertoire that reacts to RT-based peptides, it is a distinct possibility that the hydroxyl group of P1-Tyr could make additional favorable hydrogen bond interactions with the TCR that would not be permitted with a phenylalanine or isoleucine at P1. Such interactions could potentially increase the affinity or time of engagement of the TCR-MHC interaction, which could in turn enhance the T cell-mediated immune response.

A second feature of the A2/I1Y complex that differentiates it from the I1F and RT complexes and may be involved in TCR interactions is the interaction between the P1-Tyr and P4-Glu. Comparison of the crystallographic structures of the A6 TCR/Tax peptide/A2 complex *versus* the Tax/A2 complex alone demonstrates that the middle of the Tax peptide undergoes a significant conformational change upon TCR binding (11). This

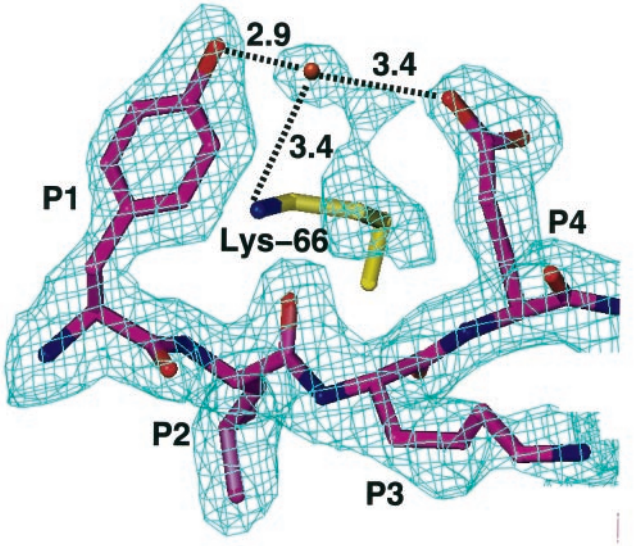

FIG. 4. **Hydrogen bond interactions bridged by water between the P1 tyrosine and the P4 glutamate affect peptide rigidity.** The I1Y peptide is shown in *magenta,* and the Lys-66 residue of the A2 α1 α-helix is shown in *yellow*. Other A2 binding cleft residues have been omitted for clarity. In this orientation, the α1-helix is behind the plane of the page and the α2-helix is in front of the plane of the page. Lys-66 is behind the plane of the page and behind the electron density that presumably reflects relatively ordered waters. The averaged omit map (*green*) is contoured at 1.1 σ with a 1.0-Å cover radius. The area of density between P1 and P4 is oriented perpendicular to the peptide backbone with the upper portion of density lying behind the plane of the page with the lower portion of the density in front of the plane of the page. This density could accommodate up to three waters. The potential position of one water is indicated by a *red sphere* with the distances from this water to the P1 tyrosine, P4 glutamate, and Lys-66 residues indicated.

suggests that some degree of conformational flexibility in the bound peptide may be required for engagement of the TCR by the MHC complex. The additional hydrogen bond interaction of the P4-glutamate of the I1Y peptide with the P1-Tyr should make the bound peptide more rigid than the I1F and RT peptides, a factor that could easily alter T cell recognition. For example, in the co-crystal structure of the TCR 2C and H-2K^b-dEV8, there are six contacts between four residues on the CDR3α loop with the P4 residue (26).

In summary, our data suggest that some of the increased immunogenicity of the A2/I1Y complex is due to the increased peptide-MHC affinity afforded by the aromatic substitution at P1. At least part of the mechanism is due to increases in the concentration of cell surface peptide-MHC and involves the avidity of the MHC-peptide-TCR interaction. The modeling of the TCR contacts and the differing biological reactivity between A2/I1F and A2/I1Y suggests that the interactions between the MHC and TCR are also affected. Thus, some part of the increased immunogenicity must be due to increased affinity (or duration of contact) between the peptide-MHC and the TCR. The increases in immunological reactivity of I1Y and I1F peptides are most likely due to a combination of equilibrium mechanisms due to the increase in the density of complexes at the cell surface and thermodynamic (or kinetic) mechanisms due to the changes in the interface of MHC-peptide and TCR. As these types of changes cannot easily be anticipated, altered peptide ligands designed for immunotherapy must be carefully examined biologically to test the effects of the changes made to the peptide.

TABLE II
Distances between atoms in residues of TCR models and peptide P1 residues

Atom of Met-28	RT [C(δ)]	I1F [C(ζ)]	I1Y [OH]
A. B7-TCR[a]			
C(ϵ)	5.94	4.62	4.06
S(δ)	5.15	3.66	3.08
C(γ)	3.73	2.11	1.38
C(β)	4.59	2.99	1.75
C(α)	4.29	3.00	1.98
N	5.37	4.27	3.37
C	4.79	3.55	2.45
O	4.46	3.23	2.25
Atom of Gly-28	**RT [C(δ)]**	**I1F [C(ζ)]**	**I1Y [OH]**
B. A6-TCR			
C(α)	4.32	2.94	1.88
N	5.62	4.30	3.24
C	4.62	3.30	2.13
O	4.03	2.82	1.91

[a] Interatomic distances between α chain Met-28 of B7-TCR and the closest atom of the peptide P1 residue. Distances (Å) below the optimal van der Waals contact distance (after factoring in coordinate error) are underlined.

[b] Interatomic distances between α chain Gly-28 of A6-TCR and the closest atom of the peptide P1 residue. Distances (Å) that are below the optimal van der Waals contact distance (after factoring in coordinate error) are underlined.

Acknowledgments—We thank Dr. Michael Batalia and Jennifer Kuhns for assistance in data collection and Dr. Rui Zhao for expert crystallographic assistance as well as critical reading of this manuscript. We also thank all members of our laboratories for excellent discussions.

REFERENCES

1. Doherty, P. C., Allan, W., Eichelberger, M., and Carding, S. R. (1992) *Annu. Rev. Immunol.* **10,** 123–151
2. Zinkernagel, R. M., and Doherty, P. C. (1974) *Nature* **248,** 701–702
3. Schmitz, J. E., Kuroda, M. J., Santra, S., Sasseville, V. G., Simon, M. A., Lifton, M. A., Racz, P., Tenner-Racz, K., Dalesandro, M., Scallon, B. J., Ghrayeb, J., Forman, M. A., Montefiori, D. C., Rieber, E. P., Letvin, N. L., and Reimann, K. A. (1999) *Science* **283,** 857–860
4. Batalia, M. A., and Collins, E. J. (1997) *Biopolymers* **43,** 281–302
5. Madden, D. R., Garboczi, D. N., and Wiley, D. C. (1993) *Cell* **75,** 693–708
6. Jardetzky, T. S., Lane, W. S., Robinson, R. A., Madden, D. R., and Wiley, D. C. (1991) *Nature* **353,** 326–329
7. Hunt, D. F., Henderson, R. A., Shabanowitz, J., Sakaguchi, K., Michel, H., Sevilir, N., Cox, A. L., Appella, E., and Engelhard, V. H. (1992) *Science* **255,** 1261–1263
8. Falk, K., Rotzschke, O., Stevanovic, S., Jung, G., and Rammensee, H. G. (1991) *Nature* **351,** 290–296
9. Ruppert, J., Sidney, J., Celis, E., Kubo, R. T., Grey, H. M., and Sette, A. (1993) *Cell* **74,** 929–37
10. Pogue, R. R., Eron, J., Frelinger, J. A., and Matsui, M. (1995) *Proc. Natl. Acad. Sci. U. S. A.* **92,** 8166–8170
11. Garboczi, D. N., Ghosh, P., Utz, U., Fan, Q. R., Biddison, W. E., and Wiley, D. C. (1996) *Nature* **384,** 134–141
12. Ding, Y. H., Smith, K. J., Garboczi, D. N., Utz, U., Biddison, W. E., and Wiley, D. C. (1998) *Immunity* **8,** 403–411
13. Garboczi, D. N., Hung, D. T., and Wiley, D. C. (1992) *Proc. Natl. Acad. Sci. U. S. A.* **89,** 3429–3233
14. Bouvier, M., and Wiley, D. C. (1994) *Science* **265,** 398–402
15. Otwinowski, Z., and Minor, W. (1996) *Methods Enzymol.* **276,** 307–326
16. Dodson, E. J., Winn, M., and Ralph, A. (1998) *Methods Enzymol.* **277,** 620–633
17. Cowtan, K. (1994) *Joint CCP4 and ESF-EACBM Newsletter on Protein Crystallography* **31,** 34–38
18. Jones, T. A., Zou, J.-Y., Cowan, S. W., and Kjeldgaard, M. (1991) *Acta Crystallogr. Sect. A Struct. Crystallogr. Cryst. Chem.* **47,** 110–119
19. Brunger, A. (1992) *X-PLOR, A System for X-ray Crystallography and NMR,* Version 3.1, Yale University Press, New Haven, CT
20. Murshudov, G. N., Vagin, A. A., and Dodson, E. J. (1997) *Acta Crystallogr. Sect. D Struct. Sci.* **53,** 240–255
21. Dodson, E. J., Winn, M., and Ralph, A. (1997) *Methods Enzymol.* **277,** 620–633
22. Lamzin, V. S., and Wilson, K. S. (1997) *Methods Enzymol.* **277,** 269–305
23. Brunger, A. T. (1992) *Nature* **355,** 472–474
24. Morgan, C. S., Holton, J. M., Olafson, B. D., Bjorkman, P. J., and Mayo, S. L. (1997) *Protein Sci.* **6,** 1771–1773
25. Burley, S. K., and Petsko, G. A. (1985) *Science* **229,** 23–28
26. Garcia, K. C., Degano, M., Pease, L. R., Huang, M., Peterson, P. A., Teyton, L., and Wilson, I. A. (1998) *Science* **279,** 1166–2272